Advances in Dynamical Systems and Applications
ISSN 0973-5321, Volume 12, Number 2, pp. 63–83 (2017)
http://campus.mst.edu/adsa

Persistence and Bifurcation in a Two-Dimensional Discrete System

Ziyad AlSharawi
American University of Sharjah
Department of Mathematics and Statistics
P.O. 26666, University City, Sharjah, UAE
zsharawi@aus.edu

Sourav Kumar Sasmal and **Joydev Chattopadhyay**
Indian Statistical Institute
Agricultural and Ecological Research Unit
203 B.T. Road, Kolkata, 700108, India
joydev@isical.ac.in

Abstract

In this paper, we consider a planar discrete system with some negative coefficients, then investigate its positive solutions. We characterize boundedness and persistence of the system. Under certain conditions on the parameters, we show that the system undergoes a Neimark–Sacker bifurcation and the obtained invariant curve is supercritical.

AMS Subject Classifications: 65Q10, 39A30, 39A28.
Keywords: Discrete systems, persistence, planar maps, Neimark–Sacker bifurcation.

1 Introduction

Discrete-time systems of the form

$$\begin{cases} x_{n+1} = & F(x_n, y_n) \\ y_{n+1} = & G(x_n, y_n) \end{cases}$$

generate the dynamics obtained by iterating the planar maps F and G, which are widely used throughout literature. The primary motivation for studying such systems stems from

Received February 11, 2017; Accepted June 26, 2017
Communicated by Mustafa R. S. Kulenović

biological and ecological reasons since they provide a realistic approach toward modeling the behaviour of species with nonoverlapping generations [2, 4, 7, 15]. In general, the qualitative features of the maps F and G are determined by the nature of interaction among and between the studied species. For instance, there are three main types of interspecific interactions, namely predator-prey interaction, competition interaction and the third is mutualism (or symbiosis). In a discrete-time predator-prey model [4, 16], F and G satisfy $F(\uparrow,\downarrow)$ while $G(\uparrow,\uparrow)$, where we use $\uparrow$ to represent the nondecreasing property while $\downarrow$ represents the nonincreasing property. A classical example of this type is given by Nicholson–Baily model [4, 17] in which $F(x,y) = \lambda x f(x,y) = \alpha x e^{-ay}$ and $G(x,y) = \beta x g(x,y) = \beta x(1-e^{-ay})$. In a discrete-time competition model, F and G can be taken to satisfy $F(\uparrow,\downarrow)$ while $G(\downarrow,\uparrow)$ [10, 14, 18]. The Leslie–Gower model [14] is a well-known prototype of this scenario in which $F(x,y) = xf(x,y) = \alpha x/(1+a_{11}x+a_{12}y)$ and $G(x,y) = yf(x,y) = \beta y/(1+a_{21}x+a_{22}y)$. Finally, in mutualism both species benefit from the interaction [5, 6, 20]; however, modeling this type of interaction is getting little attention in continuous models, and almost no attention in discrete models. In discrete models of mutualism [6], F and G can be taken to satisfy $F(\uparrow,\uparrow)$ while $G(\uparrow,\uparrow)$, and therefore, the dynamics of such systems can be simple. A deviation from the aforementioned monotonic maps leads to considering maps F and G that are monotonic for a restricted parameter set and on a subset of the state space. This change in monotonicity leads to more complicated dynamics. A well-known model is the discrete-time Lotka–Volterra competition model [9, 15]

$$\begin{cases} x_{n+1} = & F(x_n,y_n) = x_n e^{r(1-x_n-by_n)} \\ y_{n+1} = & G(x_n,y_n) = y_n e^{s(1-cx_n-y_n)}. \end{cases} \tag{1.1}$$

Planar maps of this type have been given considerable attention by Smith [19]. Observe that F in (1.1) changes monotonicity in its first variable while G changes monotonicity in its second variable (i.e., $F(\curvearrowright,\downarrow)$ and $G(\downarrow,\curvearrowright)$); however, the positive quadrant is still forming an obvious invariant domain. In this study, we add another factor of complexity by considering planar maps $F(\curvearrowright,\downarrow)$ and $G(\uparrow,\uparrow)$ that have no obvious invariant domain. In particular, we consider the discrete-time system

$$\begin{cases} x_{n+1} = & F(x_n,y_n) = \dfrac{rkx_n}{k+(r-1)x_n} - \alpha x_n y_n \\ y_{n+1} = & G(x_n,y_n) = \beta x_n y_n - \mu y_n, \end{cases} \tag{1.2}$$

where the parameters $k, \alpha, \beta > 0$ and $r > 1$. Although this system can be connected to certain continuous predator-prey models, our interest here is limited to its abstract dynamics, and in particular, the asymptotic behaviour of its positive solutions, which contributes toward understanding the dynamics of discrete planar systems in general. To reduce the number of parameters, we let $x_n = \dfrac{k}{r-1}X_n$ and $y_n = \dfrac{1}{\alpha}Y_n$, then define

$\widetilde{B} := \beta k$ and $B := \dfrac{\widetilde{B}}{r-1}$. Thus, we obtain the system

$$\begin{cases} X_{n+1} = & X_n \left(\dfrac{r}{1+X_n} - Y_n \right) \\ \\ Y_{n+1} = & Y_n \left(BX_n - \mu \right). \end{cases} \tag{1.3}$$

For our writing convenience, we ignore the upper case symbols and consider

$$f(x) = \frac{r}{1+x} \quad \text{while} \quad g(x) = (Bx - \mu)$$

to obtain the system

$$\begin{cases} x_{n+1} = & F(x_n, y_n) = x_n \left(f(x_n) - y_n \right) \\ y_{n+1} = & G(x_n, y_n) = y_n g(x_n), \end{cases} \tag{1.4}$$

where $r > 1$ and $B, \mu > 0$.

This paper is organized as follows: In section two, we discuss the local stability of equilibria. In section three, we eliminate x_n and establish an invariant region with respect to y_n. Furthermore, we show the existence of periodic solutions. In section four, we discuss the boundedness and persistence of solutions. A rigours analysis is done in section five to prove the existence of Neimark–Sacker bifurcation.

2 Equilibrium Solutions and Local Stability

System (1.4) has a total of three equilibrium points, namely $E_0 := (0,0)$, $E_1 := (r-1, 0)$ and

$$E_* = (\bar{x}_1, \bar{y}_1) = \left(g^{-1}(1), f(g^{-1}(1)) - 1 \right) = \left(\frac{1+\mu}{B}, \frac{Br}{B+\mu+1} - 1 \right).$$

We denote E_0 and E_1 as the boundary equilibria while E_* as the interior or positive one. The local stability of an equilibrium $E = (\overline{x}, \overline{y})$ can be determined by the eigenvalues λ_i, $i = 1, 2$ of the following Jacobian matrix evaluated at an equilibrium.

$$J(\bar{x}, \bar{y}) = \begin{bmatrix} \bar{x} f'(\bar{x}) + f(\bar{x}) - \bar{y} & -\bar{x} \\ B\bar{y} & g(\bar{x}) \end{bmatrix}.$$

It is obvious that the boundary equilibria are not within the positive solutions that we are interested in; however, we investigate their local stability to have full understanding of the dynamics. Observe that we must have $x_n > \dfrac{\mu}{B}$ for all n. Furthermore, if $y_n = 0$,

then x_n stabilizes at the positive equilibrium of $x_{n+1} = \dfrac{rx_n}{1+x_n}$, i.e., $\bar{x} = r-1$. Now, the boundary equilibrium E_0 has the eigenvalues $\lambda_1 = r > 1$ and $\lambda_2 = -\mu < 0$. Thus, E_0 is a saddle when $0 < \mu < 1$ and a repeller when $\mu > 1$. On the other hand, the boundary equilibrium E_1 has the eigenvalues $\lambda_1 = \dfrac{1}{r} < 1$ and $\lambda_2 = B(r-1) - \mu = \tilde{B} - \mu$. Thus, E_1 is a saddle if $|\tilde{B} - \mu| > 1$ and is locally asymptotically stable if $|\tilde{B} - \mu| < 1$.

Next, we focus on the positive equilibrium E_*. Observe that to have $\bar{y}_1 > 0$, we need $\widetilde{B} > \mu + 1$. At E_*, the Jacobian matrix becomes

$$J(\bar{x}_1, \bar{y}_1) = \begin{bmatrix} \bar{x}_1 f'(\bar{x}_1) + 1 & -\bar{x}_1 \\ B\bar{y}_1 & 1 \end{bmatrix}.$$

To analyze the stability of $E_* = (\bar{x}_1, \bar{y}_1)$ with some convenience, we define $u = B\bar{x}_1\bar{y}_1$ and $v = \dfrac{r\bar{x}_1}{(1+\bar{x}_1)^2}$. We obtain $Det(J) = 1+u-v$, $Tr(J) = 2-v$ and the characteristic equation

$$\lambda^2 - (2-v)\lambda + (1+u-v) = 0.$$

Therefore, the eigenvalues are given by

$$\lambda_j = \frac{1}{2}\left(2 - v + (-1)^j\sqrt{v^2 - 4u}\right), \ j = 1, 2. \tag{2.1}$$

Our next lemma gives a characterization of the eigenvalues.

Lemma 2.1. *Let $u = B\bar{x}_1\bar{y}_1$ and $v = \dfrac{r\bar{x}_1}{(1+\bar{x}_1)^2}$. The eigenvalues are both within the unit circle if and only if (u, v) is within the triangle of vertices $(0,0), (0,2)$ and $(4,4)$. If $v > 2 + \dfrac{1}{2}u$, then $|\lambda_2| < 1$ while $|\lambda_1| > 1$.*

Proof. The region in which both eigenvalues are within the unit circle can be obtained from the Jury conditions

$$|Det(J)| < 1, \quad 1 - Tr(J) + Det(J) > 0 \quad \text{and} \quad 1 + Tr(J) + Det(J) > 0.$$

However, the expressions of λ_1 and λ_2 can be used and manipulated to conclude the location of each eigenvalue. Fig 2.1 illustrates the computational details. □

To know the impact of our original parameters in (1.4), we manipulate the regions obtained in Lemma 2.1 and write them in terms of our original parameters. We start by the case in which one of the eigenvalues is within the unit circle. The condition $v > 2 + \dfrac{1}{2}u$ translates into

$$B(\mu+1)(\mu+B-1)r < (\mu-3)(B+\mu+1)^2. \tag{2.2}$$

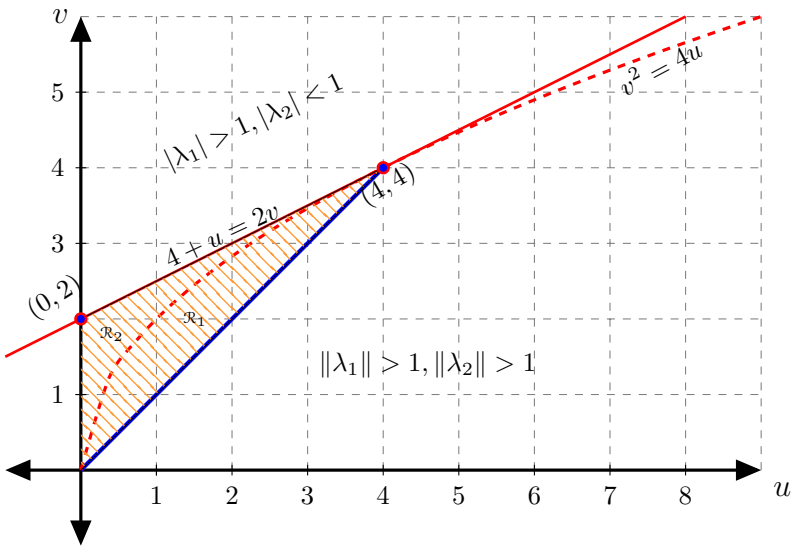

Figure 2.1: This figure illustrates the effect of the (u, v) values on the eigenvalues of the Jacobian matrix at $(\bar{x}_1, \bar{y}_1)$. The shaded R_1-region gives both eigenvalues nonreal with magnitude less than one, while the R_2-region gives both eigenvalues real with magnitude less than one. The line segment in blue between $(0, 0)$ and $(4, 4)$ is the place where both eigenvalues are nonreal of magnitude one.

However, since B depends on r, we rather consider our parameters $\tilde{B}$, r and μ. In this case, (2.2) becomes

$$P_1(\widetilde{B}) = \left[\frac{r+3}{(r-1)} + \mu\right] \widetilde{B}^2 + (1+\mu)[4+(1-\mu)(2-r)]\widetilde{B} + (3-\mu)(1+\mu)^2(r-1) < 0. \tag{2.3}$$

Now, we focus on our parameters to obtain both eigenvalues within the unit circle. The triangular region obtained in Lemma 2.1, which is determined by $0 < u < 4$ and $u < v < 2 + \frac{1}{2}u$, translates into a region determined by the inequalities

$$\begin{cases} \tilde{B} \;>\; 1+\mu, & (u > 0) \\ [\mu(r-1) + (r-5)]\,\tilde{B} \;<\; (\mu+5)(\mu+1)(r-1), & (u < 4) \\ \tilde{B}^2 + (\mu r - 2\mu - 2)\,\tilde{B} \;<\; (r-1)(\mu+1)^2, & (u < v) \\ P_1(\widetilde{B}) > 0, & (v < 2 + \frac{1}{2}u). \end{cases} \tag{2.4}$$

Notice that it is possible to solve the inequalities in (2.4) but the work is tedious; instead, it can be more convenient to consider r and $\tilde{B}$ as our major parameters while μ as a constant, then write r and $\tilde{B}$ in terms of u and v, i.e,

$$r = \frac{(\mu+u+1)^2}{(\mu+1)(u-(\mu+1)(v-1))} \quad \text{and} \quad \tilde{B} = \frac{(\mu^2 v + \mu u + 2\mu v + u^2 + u + v)}{(\mu+1)v}.$$

To have $r > 1$, we need $u > (\mu + 1)(v - 1)$, which means the shaded region of Fig. 2.1 is not completely utilized. However, the triangular region obtained in Lemma 2.1 can be traced to obtain the stability region with respect to r and $\tilde{B}$. We summarize the obtained results in the following Lemma.

Lemma 2.2. *Each of the following holds true for* (1.4)*:*

(i) If the parameters $\tilde{B}$, r and μ satisfy (2.4)*, then $(\bar{x}_1, \bar{y}_1)$ is locally asymptotically stable. Fig. 2.2 illustrates the stability region.*

(ii) If the parameters $\tilde{B}$, r and μ satisfy (2.3)*, then $(\bar{x}_1, \bar{y}_1)$ is a saddle. Again, Fig. 2.2 illustrates the feasible region.*

(iii) Both eigenvalues of the Jacobian matrix are nonreal of modulus one when

$$\tilde{B}_1 := [r, \tilde{B}] = \left[\frac{(\mu + t + 1)^2}{(\mu + 1)(1 - \mu(t - 1))}, \mu + 2 + \frac{t}{(\mu + 1)} \right],$$

where either $0 < t \leq 4,\ \mu < \dfrac{1}{3}$ which is illustrated by the blue solid-curve in Fig. 2.2 (a), or $0 < t < 1 + \dfrac{1}{\mu},\ \mu \geq \dfrac{1}{3}$ which is illustrated again by the blue solid-curve in Fig. 2.2 (b).

We give a numerical example, which together with Fig 2.2 illustrate the various cases of Lemma 2.2.

Example 2.3. (i) Consider $\mu = \dfrac{1}{10} < \dfrac{1}{3}$. We fix r and let $\tilde{B}$ change along a vertical fiber in Fig. 2.2(a)

- Fix $r = 20$:

$\tilde{B} =$	$\bar{x}_1 \approx$	$\bar{y}_1 \approx$	$\lambda_1 \approx$	$\lambda_2 \approx$
$\frac{12}{10}$	17.417	0.086	0.075	0.898
3	6.967	1.510	$-0.098 - 0.676i$	$-0.098 + 0.676i$
6	3.483	3.461	$-0.733 - 0.897i$	$-0.733 + 0.897i$

- Fix $r = 28$:

$\tilde{B} =$	$\bar{x}_1 \approx$	$\bar{y}_1 \approx$	$\lambda_1 \approx$	$\lambda_2 \approx$
$\frac{12}{10}$	24.750	0.087	0.058	0.898
3	9.900	1.569	$-0.167 - 0.604i$	$-0.167 + 0.604i$
6	4.076	3.915	$-0.957 - 0.495i$	$-0.957 + 0.495i$
10	2.970	6.053	-2.188	-1.089

- Fix $r = 50$:

$\tilde{B} =$	$\bar{x}_1 \approx$	$\bar{y}_1 \approx$	$\lambda_1 \approx$	$\lambda_2 \approx$
$\frac{12}{10}$	44.917	0.089	0.036	0.898
3	17.967	1.636	$-0.249 - 0.491i$	$-0.249 + 0.491i$
6	8.983	4.008	-2.071	-0.436
10	5.390	6.825	-4.140	-0.461

(ii) Consider $\mu = \frac{2}{5} > \frac{1}{3}$. We fix $r = 70$ and let $\tilde{B}$ change along a vertical fiber in Fig. 2.2(b)

$\tilde{B} =$	$\bar{x}_1 \approx$	$\bar{y}_1 \approx$	$\lambda_1 \approx$	$\lambda_2 \approx$
$\frac{3}{2}$	64.400	0.070	0.050	0.896
3	32.200	1.108	$-0.022 - 0.712i$	$-0.022 + 0.712i$
6	16.100	3.094	$-0.927 - 0.786i$	$-0.927 + 0.786i$
9	10.733	4.966	-2.431	-1.026
15	6.440	8.409	-5.265	-0.879
40	2.415	19.498	-11.271	-1.225

3 The y_n Equation

In this section, we eliminate x_n from our system and focus on the dynamics of y_n. This notion has the advantage of simplifying the mathematical analysis in finding an invariant region. The second equation of (1.4) gives us

$$x_n = g^{-1}\left(\frac{y_{n+1}}{y_n}\right), \tag{3.1}$$

then we obtain from the first equation

$$g^{-1}\left(\frac{y_{n+2}}{y_{n+1}}\right) = g^{-1}\left(\frac{y_{n+1}}{y_n}\right)\left(f\left(g^{-1}\left(\frac{y_{n+1}}{y_n}\right)\right) - y_n\right).$$

We simplify to obtain

$$y_{n+2} = y_{n+1}F(y_n, y_{n+1}), \quad \text{where} \quad F(x,y) = \left(rB - \frac{rB^2x}{(B+\mu)x + y} - y - \mu x - \mu\right) \tag{3.2}$$

and $x, y > 0$. We must have $F(x,y) > 0$, i.e.,

$$rB - \mu > rB\frac{Bx}{(y+\mu x) + Bx} + (y + \mu x). \tag{3.3}$$

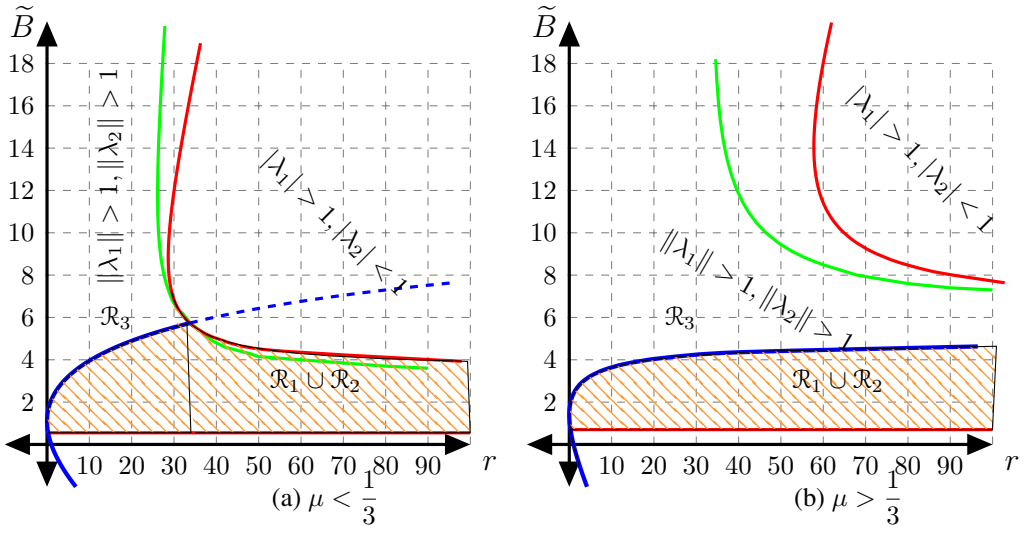

Figure 2.2: The shaded regions in both figures show the solution of (2.3). Fig. (a) has been captured at $\mu = \dfrac{1}{10}$ while Fig (b) at $\mu = \dfrac{2}{5}$. The red curve is the transformation of the line $v = 2 + \dfrac{1}{2}u$ under the constraints of our parameters. The intersection between the curves takes place when $r = \dfrac{(\mu+5)^2}{(\mu+1)(1-3\mu)}$ and $\mu < \dfrac{1}{3}$. The blue solid curve in the first quadrant represents $u = v$, which is the place where both eigenvalues are on the unit circle. At the green curve, eigenvalues change from complex to real or vice versa. The regions $\mathcal{R}_1 \cup \mathcal{R}_2$ correspond to the shaded regions in Fig. 2.1. The region $\mathcal{R}_3$ gives nonreal eigenvalues which are located out of the unit circle.

Also, it is obvious that a solution must oscillate about the curve $F(x, y) = 1$, i.e.,

$$rB - \mu - 1 = rB\frac{Bx}{(y + \mu x) + Bx} + (y + \mu x). \tag{3.4}$$

We illustrate (3.3) and (3.4) in Figure 3.1.

Denote the region in the positive quadrant that satisfies $F(x, y) > 0$ (the axes are not included) by $\mathcal{R}$, and consider the two-dimensional map $T : (y_{n-1}, y_n) \to (y_n, y_{n+1})$. In general, and as Fig 3.1 illustrates, The region $\mathcal{R}$ is not invariant under T. However, we are interested in establishing an invariant region that can be used to ensure positive solutions in our original system. We start by forcing the first obvious constraint

$$\alpha := Br - \mu < \frac{Br}{B + \mu} - 1 =: \beta. \tag{3.5}$$

Consider $\mathcal{D}$ to be the interior of the triangular region of vertices $(0, 0)$, $(\beta, 0)$ and $(0, \alpha)$. It is a simple computation to show that the upper boundary of this region satisfies

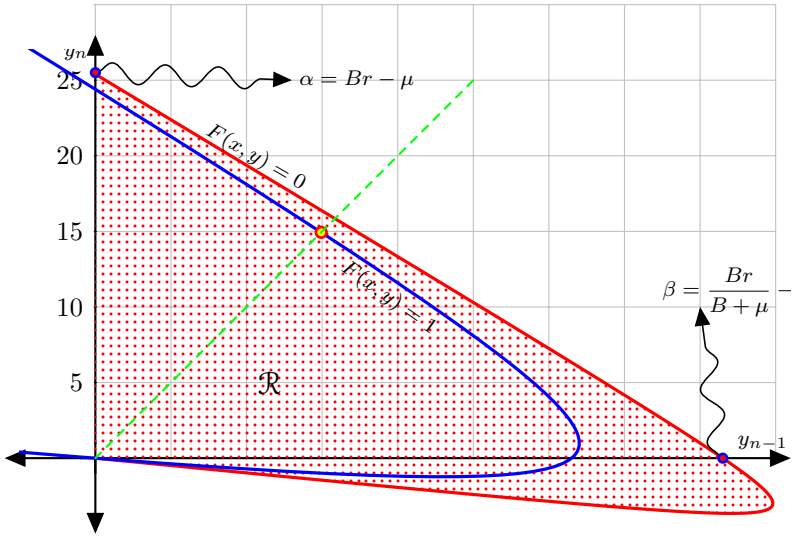

Figure 3.1: This figure illustrates the curve $F(x, y) = 1$ and the region given by $F(x, y) > 0$. The grid unit is taken to be 5 and the parameters' values are taken $\mu = \dfrac{1}{10}, r = 51$ and $\tilde{B} = 5$.

$F(x, y) \geq 0$. Hence, we have $\mathcal{D} \subset \mathcal{R}$. Now, we give the following result in the next lemma.

Lemma 3.1. *Consider* $\alpha = Br - \mu$ *and* $\beta = \dfrac{Br}{B+\mu} - 1$, *and assume that* $\tilde{B} > 1 + \mu$. *If* $\alpha(\beta + 1)^2 < 4\beta^2$, *then the region* $\mathcal{D}$ *is invariant under the map* T *defined by* $T(x, y) = (y, yF(x, y))$.

Proof. The condition $\tilde{B} > 1 + \mu$ ensures that $\bar{y}_1 > 0$, and consequently $\alpha, \beta > 0$. Also, note that the condition $\alpha(\beta + 1)^2 < 4\beta^2$ is stronger than the condition of Inequality 3. Now, let $(s, t) \in \mathcal{D}$. We have

$$0 < s < \beta \qquad \text{and} \qquad 0 < t < \frac{\alpha}{\beta}(\beta - s).$$

Since $T(s, t) = (t, tF(s, t))$, all we need is to show that

$$tF(s, t) < \frac{\alpha}{\beta}(\beta - t).$$

However, since F is decreasing in its first argument, i.e., $F(s, t) < F(0, t)$, it is sufficient to show that

$$tF(0, t) = t(\alpha - t) < \frac{\alpha}{\beta}(\beta - t).$$

This is equivalent to $\beta t^2 - \alpha(\beta + 1)t + \alpha\beta > 0$, which is valid due to the condition $\alpha(\beta + 1)^2 < 4\beta^2$. □

It is worth mentioning that we obtained an invariant region in Lemma 3.1 using relatively simple constraints on the parameters. However, it is possible to expand the region $\mathcal{D}$, but that will be on the expense of the constraints. Next, we explore the condition $\alpha(\beta+1)^2 < 4\beta^2$, which is in fact

$$\tilde{B}^3 r^3 - (r-1)(\mu r^2 + 4r^2 - 8r + 4)\tilde{B}^2 + 8\mu(r-1)^3\tilde{B} - 4\mu^2(r-1)^3 < 0.$$

The asymptotic behavior for large r is given by

$$\tilde{B}^3 + (-\mu - 4)\tilde{B}^2 + 8\tilde{B}\mu - 4\mu^2 = (\tilde{B} - \mu)(\tilde{B}^2 - 4\tilde{B} + 4\mu).$$

In Fig 3.2, we plot the region on the parameter space that satisfies the constraints in Lemma 3.1.

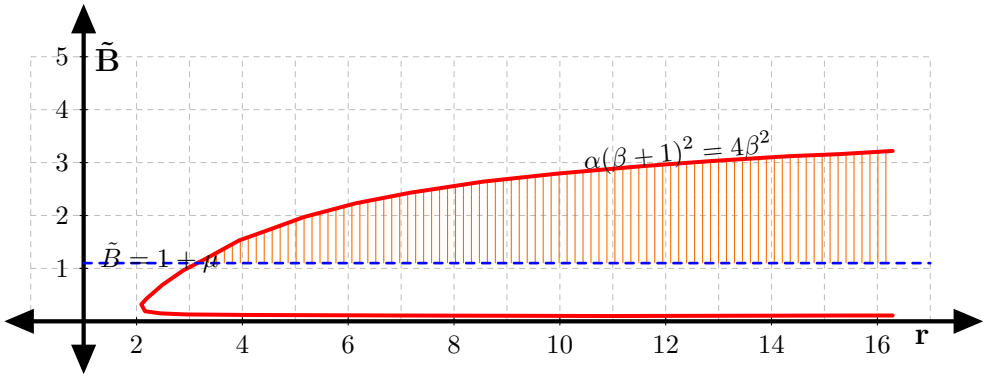

Figure 3.2: The shaded region in this figure illustrates the region that satisfies the constraints of Lemma 3.1. This figure has been captured at $\mu = \dfrac{1}{10}$.

Example 3.2. Equation (3.2) is capable of having persistent periodic solutions. For instance, if we fix $\mu = \dfrac{1}{10}$, $r = 51$ and $\tilde{B} = 5$, then we obtain the $2-periodic$ solution $\{y_0, y_1\}$, where

$$x_j = \left\{ \frac{1}{1960}\left(5275 + \sqrt{765865} - (-1)^j\sqrt{19090990 - 19750\sqrt{765865}}\right)\right\},$$

for $j = 0,\ 1$, which can be rounded to $\{y_0, y_1\} = \{2.452, 3.824\}$. Another approximate case is when we fix $\mu = 0.100$, $r = 9.942$ and $\tilde{B} = 3.999$. We obtain a $4-periodic$ solution, namely

$$[y_0, y_1, y_2, y_3] \approx [2.928, 1.144, 0.903, 1.663].$$

4 Persistence and Boundedness

Persistence is a convenient biological term that can be used to replace our usage of positive solutions, i.e., a solution $\{(x_n, y_n)\}_{n=0}^{\infty}$ of (1.4) is called persistent if $x_n, y_n > 0$ for all $n = 0, 1, \ldots$. The solution is called strongly persistent or permanent if $x_n, y_n > \delta > 0$ for all $n = 0, 1, \ldots$. Recall that when $y_n = 0$, we obtain

$$x_{n+1} = \frac{krx_n}{k + (r-1)x_n}, \tag{4.1}$$

which is in fact the Beverton–Holt model [1, 3]. The positive equilibrium $\bar{x} = k$ is a global attractor with respect to the interval $(0, \infty)$. Thus, in this case, x_n is permanent and bounded, while the persistent set is unbounded. We start by showing the boundedness of persistent solutions. From the first equation of (1.4), we obtain

$$x_{n+1} \leq \frac{rx_n}{1 + x_n} < r \quad \text{for all} \quad n \geq 0.$$

Now, from the second equation x_n must be larger than $\dfrac{\mu}{B}$, and from the first equation y_n must be less than $f(x_n)$. Thus,

$$y_n \leq f(x_n) \leq f\left(\frac{\mu}{B}\right) \quad \text{for all} \quad n \geq 0.$$

Thus, persistent solutions of (1.4) are bounded. We can strengthen this fact as follows.

Proposition 4.1. *Let* $\{(x_n, y_n)\}$ *be a persistent solution of* (1.4)*. We have* $\limsup x_n \leq r - 1$ *and* $\limsup y_n \leq \tilde{B} - \mu$.

Proof. From the first equation of (1.4), we obtain

$$x_{n+1} \leq \frac{rx_n}{1 + x_n},$$

and from which we obtain $\limsup x_n$ less than or equal to the fixed point of $f(x)$, i.e., $\limsup x_n \leq r - 1$. Next, y_n must be less than $f(x_n)$, then $y_{n+1} \leq f(x_n)g(x_n)$, and because $f(t)g(t)$ is increasing, then

$$\begin{aligned}
\limsup y_n &= \limsup y_{n+1} \\
&\leq \limsup f(x_n)g(x_n) \\
&\leq f(\limsup x_n)g(\limsup x_n) \\
&= \tilde{B} - \mu.
\end{aligned}$$

□

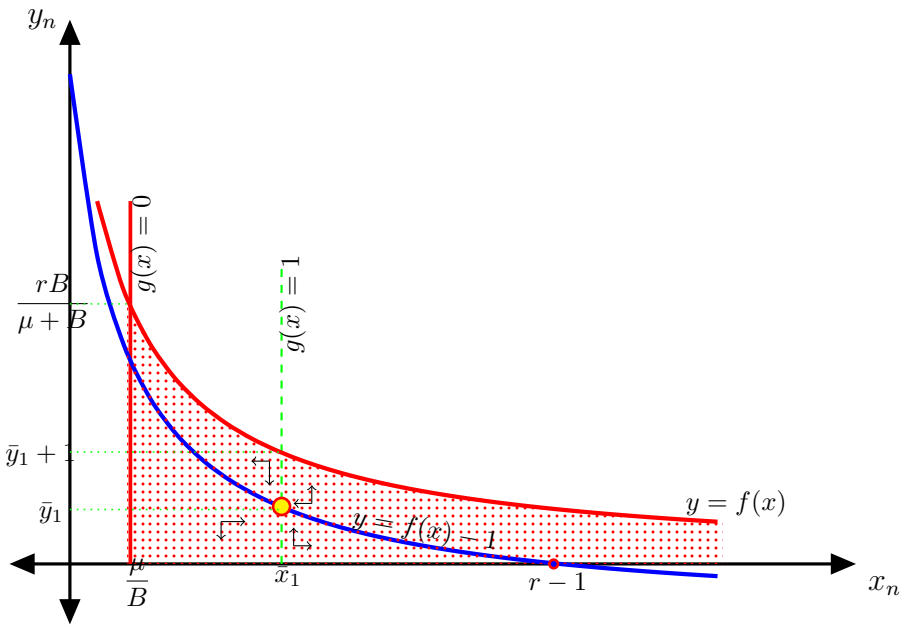

Figure 4.1: The shaded region in this figure illustrates the set of initial points that need to be investigated for possible coexistence. The curve $y = f(x) - 1$ is the nullcline (or isocline) of the prey equation while the vertical line $g(x) = 1$ is the nullcline of the predator equation.

Theorem 4.2. *No persistent solutions exist without the existence of a positive equilibrium, i.e., if* $\tilde{B} \leq \mu + 1$, *then* $y_n \to 0$ *for sufficiently large* n.

Proof. Consider $\tilde{B} \leq \mu + 1$, and assume by contrary that there exists a permanent solution $\{(x_n, y_n)\}$. If $x_n \leq r - 1$ for some $n = n_0$, then we use induction to obtain

$$x_{n+1} = x_n(f(x_n) - y_n) < x_n f(x_n) < r - 1 \quad \text{for all} \quad n \geq n_0.$$

Now, we use this fact in the second equation to obtain

$$y_{n+1} < y_n g(r-1) = y_n(B(r-1) - \mu) \leq y_n.$$

Thus, we obtained a decreasing and bounded sequence $\{y_n\}$, which must converge to either $\bar{y}_0$ or $\bar{y}_1$. This contradicts our earlier assumption. Next, we show that x_n cannot stay above $r - 1$. If x_n stays above $r - 1$, then because $r - 1 < \dfrac{\mu + 1}{B}$, we obtain $f(x_n) - y_n < 1$, and consequently x_n is decreasing. Thus, x_n must converge to a fixed point, which again leads to a contradiction. □

Corollary 4.3. *Suppose that* $\bar{y}_1 > 0$. *Either* $x_n \leq r - 1$ *for all* $n \geq n_0$ *or* y_n *is attracted to* $\bar{y}_1$.

Proof. As in the proof of Theorem 4.2, if $x_{n_0} \leq r-1$ for some $n_0 > 0$, then $x_n \leq r-1$ for all $n \geq n_0$. Next, if x_n stays above $r-1$, then

$$y_{n+1} > y_n g(r-1) > y_n.$$

Thus, y_n is increasing and bounded, and consequently must converge to $\bar{y}_1$, which completes the proof. □

We have shown in Fig. 2.2(a) and Example 2.3 that when

$$\mu < \frac{1}{3}, \quad r > \frac{(\mu+5)^2}{(\mu+1)(1-3\mu)}$$

and as we increase $\tilde{B}$, the coexistence equilibrium $(\bar{x}_1, \bar{y}_1)$ loses its stability to become a saddle. This scenario also leads to the existence of periodic solutions. We illustrate this scenario in the following example and the numerical simulations in Fig 4.2.

Example 4.4. The periodic solution of period two obtained in Example 3.2 gives a persistent solution of period two, namely $\{(x_0, y_0), (x_1, y_1)\}$, where y_0, y_1 as given in Example 3.2 and

$$x_j = \frac{1}{40}\left(-395 + \sqrt{765865} - (-1)^j \sqrt{795090 - 870\sqrt{765865}}\right), \quad j = 0, 1.$$

A rounded form of this periodic solution is $\{(2.452, 7.413), (3.824, 16.594)\}$.

Next, we focus on the bifurcation that occurs at the upper boundary of the shaded region in Fig. 2.2(a) when $r > \dfrac{(\mu+5)^2}{(\mu+1)(1-3\mu)}$. This curve is a part of the branch obtained by $4 + u = 2v$. The curve can be written in parametric form as $\tilde{B}_2 :=$

$$[r, \tilde{B}] = \left[\frac{2(t+1+\mu)^2}{(\mu+1)((1-\mu)t - 2(\mu+1))}, \frac{2t^2 + (\mu+1)(\mu+3)t + 4(\mu+1)^2}{(\mu+1)(t+4)}\right], \quad (4.2)$$

where $\dfrac{2(\mu+1)}{1-\mu} < t \leq 4$ and $0 < \mu < \dfrac{1}{3}$. Fig 4.2 shows a simulation along a curve taken slightly above this curve. The stability of the equilibrium is inherited by a cycle of length two.

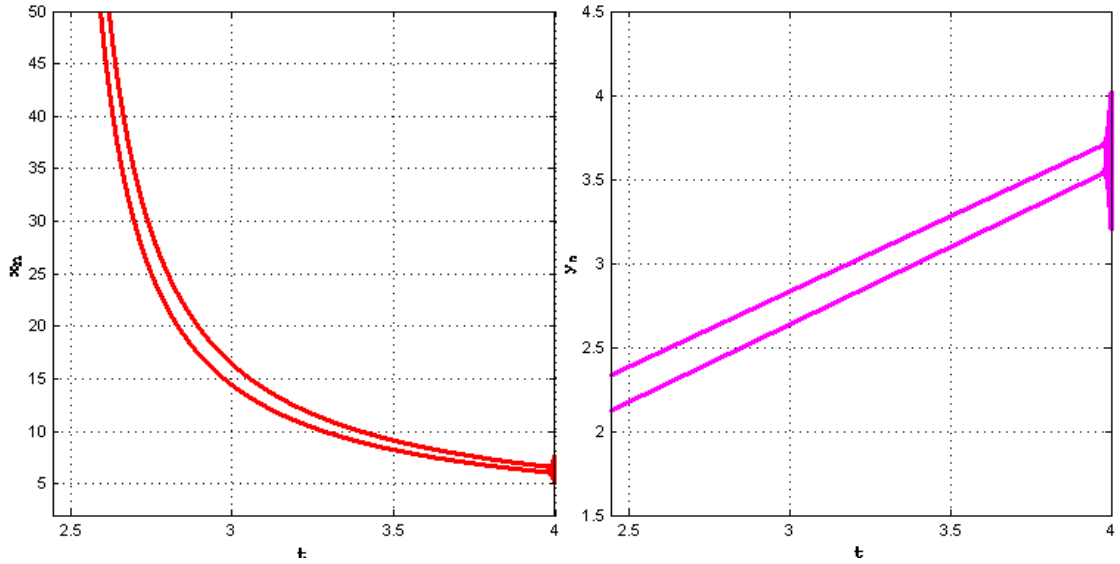

(a) The prey population x_n (b) The predator population y_n

Figure 4.2: In this figure, $\mu = 0.1$, r and $\tilde{B}$ are taken along a curve slightly above $(+0.1)$ the curve $\tilde{B}_2$ in (4.2). Observe that t is ranging over a domain that reverses and compactifies the domain of r.

5 Neimark–Sacker Bifurcation

In this section, we consider our bifurcation parameter to be $\widetilde{B}$ and focus on the positive equilibrium when the two eigenvalues (λ and $\overline{\lambda}$) of the Jacobian are nonreal and located on the unit circle. From Lemma 2.1, we need $v = u,\ 0 < u < 4$, and from Part (iii) of Lemma 2.2, we obtained a parametric form of r and $\tilde{B}$. In particular, we need to focus on the blue solid curve given in Fig. 2.2 (a) and (b), which is given by $\tilde{B}_1$ in Part (iii) of Lemma 2.2. Note that we can eliminate t and write $\tilde{B}^2+(\mu r-2\mu-2)\tilde{B}-(\mu+1)^2(r-1) = 0$, where $0 < t < 4$ implies $r > 1$ and $(\mu+1)(3\mu-1)r + (\mu+5)^2 > 0$. Observe that by considering r and $\widetilde{B}$ along the curve $\tilde{B}_1$, we already avoided $\lambda = 1$ and $\lambda^2 = 1$. In this case, the eigenvalue $\lambda := \lambda_2$ is given by

$$\lambda = \lambda_{\widetilde{B}_1} := p + \sqrt{1-p^2}\, i, \quad \text{where} \quad p = \frac{1}{2}\left(2 - B\bar{x}_1\bar{y}_1\right). \tag{5.1}$$

To avoid $\lambda^3 = 1$ and $\lambda^4 = 1$, we need

$$B\bar{x}_1\bar{y}_1 \neq 3 \quad \text{and} \quad B\bar{x}_1\bar{y}_1 \neq 2, \quad \text{consecutively.} \tag{5.2}$$

Those conditions simplify to

$$(\mu+1)(1-2\mu)r \neq (\mu+4)^2 \quad \text{and} \quad (1-\mu^2)r \neq (\mu+3)^2.$$

Up to this end, we tested the nonhyperbolicity and the nonstrong-resonance conditions. To test the transversality condition of the Naimark–Sacker bifurcation, we need to show that

$$\frac{d}{d\widetilde{B}}\left|\lambda(\widetilde{B})\right| \neq 0 \quad \text{at} \quad \widetilde{B} = \widetilde{B}_1.$$

Indeed, we have

$$\begin{aligned}\frac{d}{d\widetilde{B}}\left|\lambda(\widetilde{B})\right|^2 =& 2\left|\lambda(\widetilde{B})\right| \frac{d}{d\widetilde{B}}\left|\lambda(\widetilde{B})\right| \\ =& \frac{d}{d\widetilde{B}} Det(J(\bar{x}_1, \bar{y}_1)) \\ =& \frac{d}{d\bar{x}_1} Det\left(J\left(\bar{x}_1, \frac{r}{1+\bar{x}_1} - 1\right)\right) \frac{d\bar{x}_1}{d\widetilde{B}} \\ =& \left(\frac{-r(2+\mu+\mu\bar{x}_1)}{(1+\bar{x}_1)^3}\right)\left(\frac{-(\mu+1)(r-1)}{\widetilde{B}^2}\right) > 0.\end{aligned}$$

We summarize our discussion in the following result then give the main result of this section.

Lemma 5.1. *Consider*

$$[r, \tilde{B}] = \left[\frac{(\mu+t+1)^2}{(\mu+1)(1-\mu(t-1))}, \mu+2+\frac{t}{(\mu+1)}\right], \quad 0 < t < 4.$$

If $(\mu+1)(1-2\mu)r \neq (\mu+4)^2$ *and* $(1-\mu^2)r \neq (\mu+3)^2$, *then* $\lambda^k \neq 1$ *for* $k = 1, 2, 3$ *and* 4. *Furthermore,*

$$\frac{d}{d\widetilde{B}}\left|\lambda(\widetilde{B})\right| \neq 0 \quad \textit{at} \quad \widetilde{B} = \widetilde{B}_1.$$

Theorem 5.2. *Consider* (1.4) *together with the hypotheses of Lemma 5.1. A Neimark–Sacker bifurcation occurs and the obtained invariant curve is supercritical.*

Proof. Based on Lemma 5.1, all we need is to show that the bifurcation is supercritical (cf. [8, 13]). Denote $\widetilde{F}(x, y) = x(f(x) - y)$ and $\widetilde{G}(x) = yg(x)$. We shift the equilibrium $(\bar{x}_1, \bar{y}_1)$ to the origin by taking the substitution $u = x - \bar{x}_1$ and $v = y - \bar{y}_1$. The (u, v) system becomes

$$\begin{cases} u_{n+1} = & (u_n + \bar{x}_1)\left(f(u_n + \bar{x}_1) - v_n - \bar{y}_1\right) - \bar{x}_1 \\ v_{n+1} = & (v_n + \bar{y}_1)g(u_n + \bar{x}_1) - \bar{y}_1. \end{cases} \tag{5.3}$$

Now, use Taylor expansion about $(0, 0)$ to obtain

$$\begin{bmatrix} u_{n+1} \\ v_{n+1} \end{bmatrix} = J(\bar{x}_1, \bar{y}_1)\begin{bmatrix} u_n \\ v_n \end{bmatrix} + \begin{bmatrix} F(u_n, v_n) \\ G(u_n, v_n) \end{bmatrix},$$

where

$$F(u,v)=\frac{-r}{(\bar{x}_1+1)^3}u^2-uv+\frac{r}{(\bar{x}_1+1)^4}u^3-\frac{r}{(\bar{x}_1+1)}\sum_{j=4}^{\infty}\frac{(-1)^j}{(1+\bar{x}_1)^j}u^j$$

and $G(u,v)=Buv$. Next, we transform the system and put the linear part in Jordan normal form by considering

$$\begin{bmatrix} u_n \\ v_n \end{bmatrix}=Q\begin{bmatrix} U_n \\ V_n \end{bmatrix},\quad \text{where}\quad Q:=\begin{bmatrix} \frac{-1}{2}\bar{x}_1 & -\frac{q}{B\bar{y}_1} \\ 1 & 0 \end{bmatrix}.$$

In this case, we obtain

$$\begin{bmatrix} U_{n+1} \\ V_{n+1} \end{bmatrix}=\begin{bmatrix} p & -\sqrt{1-p^2} \\ \sqrt{1-p^2} & p \end{bmatrix}\begin{bmatrix} U_n \\ V_n \end{bmatrix}+Q^{-1}\begin{bmatrix} F_1(U_n,V_n) \\ G_1(U_n,V_n) \end{bmatrix},$$

where

$$\begin{aligned} Q^{-1}\begin{bmatrix} F_1 \\ G_1 \end{bmatrix}&=\begin{bmatrix} 0 & 1 \\ -\frac{B\bar{y}_1}{q} & -\frac{B\bar{x}_1\bar{y}_1}{2q} \end{bmatrix}\begin{bmatrix} F(-\frac{1}{2}\bar{x}_1U-\frac{q}{B\bar{y}_1}V,U) \\ G(-\frac{1}{2}\bar{x}_1U-\frac{q}{B\bar{y}_1}V,U) \end{bmatrix}\\ &=\begin{bmatrix} -\frac{1}{2}(1+\mu)U^2-\frac{q}{y}UV \\ C_1U^2+C_2V^2+C_3UV+C_4U^3+C_5V^3+C_6UV^2+C_7VU^2 \end{bmatrix}\end{aligned}$$

and

$$C_1:=\frac{(1-p)}{2q}\left(\frac{2}{r}(1-p)(\bar{y}_1+1)+\mu-1\right),\quad C_2:=\frac{q}{r}(1+\bar{y}_1),$$

$$C_3:=\frac{2}{r}(1-p)(\bar{y}_1+1)+\frac{1}{2}(\mu-1),\quad C_4:=\frac{(1-p)^3}{qr},$$

$$C_5:=\frac{(1-p^2)}{r},\quad C_6:=\frac{3q}{r}(1-p),\quad C_7:=\frac{3}{r}(1-p)^2.$$

Thus, we need to investigate the expression

$$A(r,\widetilde{B})=\mathrm{Re}\left(\frac{(1-2\lambda)\bar{\lambda}^2}{1-\lambda}C_{11}C_{20}\right)+\frac{1}{2}|C_{11}|^2+|C_{02}|^2-\mathrm{Re}\left(\bar{\lambda}C_{21}\right)\tag{5.4}$$

at the shifted equilibrium $(0,0)$, where

$$[r,\tilde{B}]=\left[\frac{(\mu+t+1)^2}{(\mu+1)(1-\mu(t-1))},\mu+2+\frac{t}{(\mu+1)}\right],\quad 0<t<4$$

and

$$\begin{aligned} C_{20} =& \frac{1}{8}\left[F_{UU} - F_{VV} + 2G_{UV} + i(G_{UU} - G_{VV} - 2F_{UV})\right] \\ =& \frac{1}{8}\left(2C_3 - \mu - 1 + 2(C_1 - C_2 + \frac{q}{\bar{y}_1})i\right), \end{aligned}$$

$$\begin{aligned} C_{11} =& \frac{1}{4}\left[F_{UU} + F_{VV} + i(G_{UU} + G_{VV})\right] \\ =& \frac{1}{4}\left(-1 - \mu + 2(C_1 + C_2)i\right), \end{aligned}$$

$$\begin{aligned} C_{02} =& \frac{1}{8}\left[F_{UU} - F_{VV} - 2G_{UV} + i(G_{UU} - G_{VV} + 2F_{UV})\right] \\ =& \frac{1}{8}\left(-2C_3 - \mu - 1 + 2(C_1 - C_2 - \frac{q}{\bar{y}_1})i\right), \end{aligned}$$

$$\begin{aligned} C_{21} =& \frac{1}{16}\left[F_{UUU} + F_{UVV} + G_{UUV} + G_{VVV} + i(G_{UUU} + G_{UVV} - F_{UUV} - F_{VVV})\right] \\ =& \frac{1}{8}\left(C_7 + 3C_5 + (3C_4 + C_6)i\right). \end{aligned}$$

Now, we have

$$\frac{(1-2\lambda)\bar{\lambda}^2}{1-\lambda} = 2p^2 - p - \frac{3}{2} + \frac{q(1-6p+4p^2)}{2(1-p)}i. \tag{5.5}$$

By substituting in the expression of A given in (5.4), we obtain a gigantic expression in which handling by hand is a formidable task. But, we manipulate the expression using Computer Algebra System such as MAPLE[1] to obtain a simple expression written in terms of $\bar{y}_1, \mu$ and r. Here, we give the main steps. Substitute the expressions of $C_j,\ j = 1, \ldots, 7$ in C_{20}, C_{11}, C_{02} and C_{21}, then together with the expression of (5.5), we substitute in the expression of (5.4) to obtain the A-expression in terms of $(p, q, \bar{y}_1, \mu, r)$. Multiply the expression by the positive quantity $64(1-p)q^2r^2y^2$ to get rid of the denominator, then substitute $q = \sqrt{1-p^2}$. Factor out the positive quantity $(1+p)(1-p)^2$ and ignore it to obtain an expression in terms of $(p, \bar{y}_1, \mu, r)$. Next, substitute $p = \frac{1}{2}(2 - (\mu+1)\bar{y}_1)$, then factor out the positive quantity $8\bar{y}_1^2$ and ignore it to obtain the following expression in terms of $(\bar{y}_1, \mu, r)$:

$$[2\bar{y}_1 + (3\mu r + 4)](\mu+1)\bar{y}_1^2 + [\mu^2(\mu+1)r^2 + (3\mu^2 + 2\mu - 2)r + 2(\mu+1)]\bar{y}_1 - r(\mu(r-2) - 1). \tag{5.6}$$

[1]The MAPLE commands used to manipulate the expression are available at www.alsharawi.info

From the condition that puts the eigenvalues on the unit circle, i.e., $B\bar{x}_1\bar{y}_1 = (\mu+1)\bar{y}_1 = \dfrac{r\bar{x}_1}{(1+\bar{x}_1)^2}$, we obtain

$$\bar{y}_1^2 = r - 1 - (2+\mu r)\bar{y}_1.$$

Now, substitute $r - 1 - (2+\mu r)\bar{y}_1$ for $\bar{y}_1^2$ in the A-expression, then again isolate $\bar{y}_1^2$ and substitute to obtain

$$sign(A) = sign\left(r(\mu(\mu+2)\bar{y}_1 + \mu(\mu r+1) + 1 - \mu^2)\right) = +.$$

□

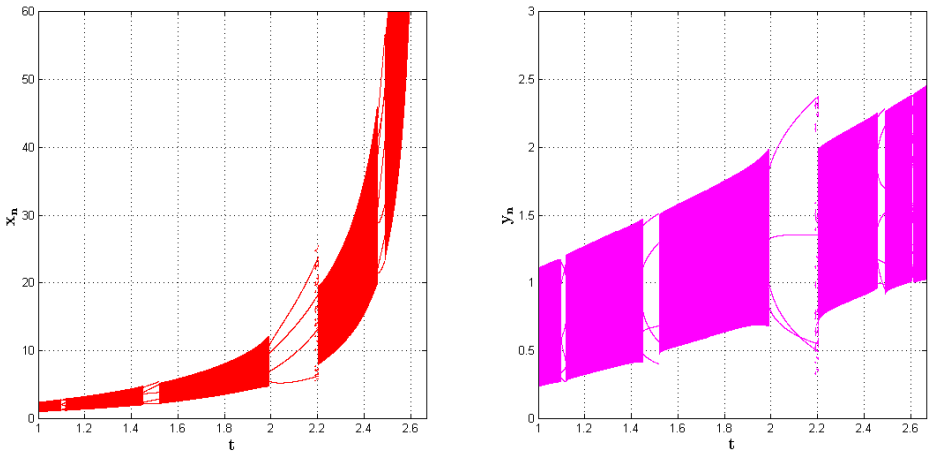

(a) The prey population x_n (b) The predator population y_n

Figure 5.1: Those figures illustrate the bifurcation that takes place when the equilibrium $(\bar{x}_1, \bar{y}_1)$ loses its stability. To be more specific, the plot is taken for orbits near the equilibrium when $\mu = 0.6$, $1 < t < \min\left\{4, 1 + \dfrac{1}{\mu}\right\}$, $r(t) = \dfrac{(\mu+t+1)^2}{(\mu+1)(1-\mu(t-1))}$ and $\tilde{B}(t) = \mu + 2 + \dfrac{t}{(\mu+1)} + 0.1$. In other words, the horizontal axis represents a perturbation (from above) of the blue-solid curve in Fig. 2.2 (b).

The densely shaded regions in figures 5.1a and 5.1b are representing the invariant curve obtained through the Neimark–Sacker bifurcation. To illustrate that, we consider $\mu = 0.6$, $\tilde{B} = 4.0$, $r = 35.0$ and plot the curve in Fig 5.2.

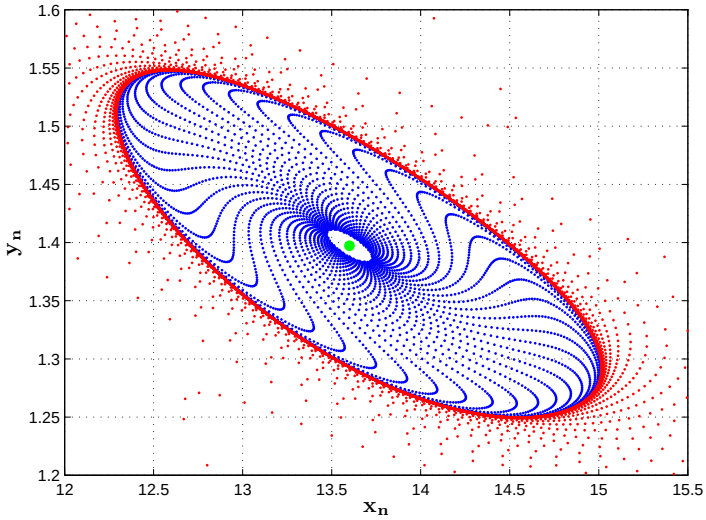

Figure 5.2: This figure shows the invariant curve obtained through a Neimark–Sacker bifurcation. The red orbit is taken for an orbit starting outside of the curve while the blue one is taken for an orbit inside the curve. The values of the parameters are $\mu = 0.6,\ \tilde{B} = 4.0$ and $r = 35.0$.

Remark 5.3. Based on the local stability result in Lemma 2.2 and the Neimark–Sacker bifurcation obtained in this section, we summarize the following: If $\mu > \frac{1}{3}$, then increasing the parameter $\widetilde{B}$ through $\widetilde{B}_1$ leads to $(\bar{x}_1, \bar{y}_1)$ losing its stability and to the creation of a stable invariant curve around $(\bar{x}_1, \bar{y}_1)$. However, if $\mu < \frac{1}{3}$, then increasing $\widetilde{B}$ through $\widetilde{B}_1$ under the condition $r < \dfrac{(\mu+5)^2}{(\mu+1)(1-3\mu)}$ leads to $(\bar{x}_1, \bar{y}_1)$ losing its stability and to the creation of a stable invariant curve around $(\bar{x}_1, \bar{y}_1)$, while increasing $\widetilde{B}$ through $\widetilde{B}_1$ under the condition $r > \dfrac{(\mu+5)^2}{(\mu+1)(1-3\mu)}$ leads to $(\bar{x}_1, \bar{y}_1)$ losing its stability without a Neimark–Sacker bifurcation. Finally, it is possible to depend on some recent results in the literature [11, 12, 16] and investigate the characteristics of the invariant curve assured by Theorem 5.2.

Acknowledgement

The first author is partially supported by a seed grant offered by the American University of Sharjah. SKS's research is supported by the postdoctoral fellowship from National Board of Higher Mathematics, Department of Atomic Energy, Government of India.

References

[1] Ziyad AlSharawi and Mohamed B. H. Rhouma. The Beverton-Holt model with periodic and conditional harvesting. *J. Biol. Dyn.*, 3(5):463–478, 2009.

[2] J. R. Beddington, C. Free, and J. Lawton. Dynamic complexity in predator–prey models framed in difference equations. *Nature*, 255:58–60, 1975.

[3] R. J. H. Beverton and S. J. Holt. *On the Dynamics of Exploited Fish Populations*. The Blackburn Press, New Jersey, 2004.

[4] L. Edelstien-Keshet. *Mathematical Models in Biology*. SIAM, Philadelphia, 2005.

[5] B. S. Goh. Stability in models of mutualism. *Amer. Natur.*, 113(2):261–275, 1979.

[6] K. Gopalsamy and Pingzhou Liu. On a discrete model of mutualism. In *New developments in difference equations and applications (Taipei, 1997)*, pages 207–216. Gordon and Breach, Amsterdam, 1999.

[7] M. P. Hassell and R. M. May. Stability in insect host-parasite models. *The Journal of Animal Ecology*, 42(3):693–726, 1973.

[8] G. V. D. Heijden. Hopf bifurcation. In *Encyclopedia of Nonlinear Science*, pages 421–424. Routledge, New York, 2005.

[9] Hong Jiang and Thomas D. Rogers. The discrete dynamics of symmetric competition in the plane. *J. Math. Biol.*, 25(6):573–596, 1987.

[10] F. G. W. Jones and J. N. Perry. Modelling populations of cyst-nematodes (nematoda: Heteroderidae). *Journal of Applied Ecology*, 15(2):349–371, 1978.

[11] T. Khyat, M. R. S. Kulenović, and E. Pilav. The invariant curve caused by naimark-sacker bifurcation of a perturbed beverton-holt difference equation. *International J. Difference Equ., in press*.

[12] T. Khyat, M. R. S. Kulenović, and E. Pilav. The Naimark-Sacker bifurcation and symptotic approximation of the invariant curve of a certain difference equation. *J. Comput. Anal. Appl.*, 23(8):1335–1346, 2017.

[13] Yuri A. Kuznetsov. *Elements of applied bifurcation theory*, volume 112 of *Applied Mathematical Sciences*. Springer-Verlag, New York, third edition, 2004.

[14] P. H. Leslie and J. C. Gower. The properties of a stochastic model for two competing species. *Biometrika*, 45:316–330, 1958.

[15] Robert M. May. Biological populations with nonoverlapping generations: Stable points, stable cycles, and chaos. *Science*, 186(4164):645–647, 1974.

[16] Kouichi Murakami. The invariant curve caused by Neimark-Sacker bifurcation. *Dyn. Contin. Discrete Impuls. Syst. Ser. A Math. Anal.*, 9(1):121–132, 2002.

[17] J. D. Murray. *Mathematical biology*, volume 19 of *Biomathematics*. Springer-Verlag, Berlin, 1989.

[18] Anthony G. Pakes and Ross A. Maller. *Mathematical ecology of plant species competition*, volume 10 of *Cambridge Studies in Mathematical Biology*. Cambridge University Press, Cambridge, 1990. A class of deterministic models for binary mixtures of plant genotypes.

[19] H. L. Smith. Planar competitive and cooperative difference equations. *J. Differ. Equations Appl.*, 3(5-6):335–357, 1998.

[20] B. Stadler and T. Dixon. *Mutualism: ants and their insect partners*. Cambridge University Press, New York, 2008.